







Electrospray ionization tandem mass spectrometry of 4-aryl-3,4-dihydrocoumarins

Herbert J. Dias^{1,2}  | William H. Santos³ | Luis C. S. Filho³  |
Eduardo J. Crevelin¹  | J. Scott McIndoe⁴  | Ricardo Vessecchi¹  |
Antônio E. M. Crotti¹ 

¹Department of Chemistry, Faculty of Philosophy, Science and Letters at Ribeirão Preto, University of São Paulo, Ribeirão Preto, Brazil

²Goiano Federal Institute of Education, Science, and Technology, Campus Urutaí, Urutaí, Brazil

³Department of Chemistry, Faculty of Sciences at Bauru, São Paulo State University, Bauru, Brazil

⁴Department of Chemistry, University of Victoria, Victoria, British Columbia, Canada

Correspondence

Antônio E. M. Crotti, Department of Chemistry, Faculty of Philosophy, Science and Letters at Ribeirão Preto, University of São Paulo, 14040-901 Ribeirão Preto, Brazil.
Email: millercrotti@ffclrp.usp.br

Funding information

National Council for Scientific and Technological Development, Grant/Award Number: 310648/2022-0; São Paulo Research Foundation, Grant/Award Numbers: 13/20094-0, 16/03036-4

Abstract

We have investigated the gas-phase fragmentation reactions of 11 synthetic 4-aryl-3,4-dihydrocoumarins by electrospray ionization tandem mass spectrometry (ESI-MS/MS) on a quadrupole-time-of flight (Q-TOF) hybrid mass spectrometer. We have also estimated thermochemical data for the protonated coumarins (precursor ion **A**) and product ion structures by computational chemistry at a B3LYP level of theory to establish the ion structures and to rationalize the fragmentation pathways. The most abundant ions in the product ion spectra of coumarins **1–11** resulted from $C_8H_8O_2$, CO_2 , $C_4H_4O_3$, $C_8H_{10}O_3$, $C_8H_8O_2$, and CH_3OH eliminations through retro-Diels–Alder (RDA) reactions, remote hydrogen rearrangements (β -eliminations), and β -lactone ring contraction. Although the investigated coumarins shared most of the fragmentation pathways, formation of a benzylic product ion and its corresponding tropylium ion was diagnostic of the substituents at ring C. The thermochemical data revealed that the nature and position of the substituents at ring C played a key role in the formation of this product ion and determined its relative intensity in the product ion spectrum. The results of this study contribute to knowledge of the gas-phase ion chemistry of this important class of organic compounds.

KEYWORDS

arylcoumarins, benzylic ions, computational chemistry, electronic effects, tropylium ions

1 | INTRODUCTION

The term “coumarin” refers to various natural and synthetic compounds bearing a benzo-2-pyrone in their structures. This term derives from *Coumarona odorata* (or *Dipteryx odorata* (Aubl.) Willd., Fabaceae), a plant species from which Vogel isolated the first coumarin in 1820.¹ Coumarins occur naturally in some plant families,¹ mostly in Apiaceae, Asteraceae, Fabaceae, Rosaceae, Rubiaceae, Rutaceae, and Solanaceae, but these compounds can also be obtained by chemical synthesis.² The simpler synthetic coumarins were first prepared by the Perkin reaction; however, they can be synthesized by numerous methodologies, such as Pechmann and Knoevenagel reactions.^{3,4}

Coumarins display a range of biological and pharmacological behavior,^{5,6} including antitumor,^{7,8} anti-HIV,^{9–11} vasorelaxant,¹² COX-inhibitor,¹³ and anticancer¹⁴ activity. Additionally, coumarins play an essential role in the chemical industry, for example, in the production of essences, perfumes, toothpaste, plastics, synthetic rubber, insecticides, detergents, and paints.^{15–17} In particular, 4-aryl-3,4-dihydrocoumarins are important not only because they occur as neoflavonoids in some plant species^{18,19} but also because they exhibit biological properties, such as anti-inflammatory, antimicrobial, and antioxidant activities.^{20–23}

Over the last decades, electrospray ionization tandem mass spectrometry (ESI-MS/MS) has been used alone or coupled to liquid

chromatography (LC-ESI-MS/MS) as a tool to elucidate the structure of different classes of metabolites (e.g., alkaloids, neolignans, diterpenes, sesquiterpene lactones^{24–27}), including coumarins. Heinke et al identified 34 furanocoumarins in *Dorstenia gigas* and *Dorstenia foetida* leaves using LC-ESI-MS/MS. The authors showed that the technique can help to identify this class of compounds and to describe the substituent behavior, especially C₄H₈ loss in prenylated coumarins, and it could even help to establish relationships with the substitution position in the basic coumarin structure.²⁸ Liang and Han studied the fragmentation of 11 synthetic and naturally occurring coumarins isolated from *Zanthoxylum armatum* by ESI-MS/MS; they employed ion trap MSⁿ experiments to establish the fragmentation pathways and proved that different side chains in the basic coumarin structure resulted in distinct fragmentation pathways.²⁹

Borkowski et al used theoretical calculations to study the fragmentation of basic coumarins, to establish methyl radical losses in methoxylated coumarins; more specifically, they applied QTAIM and NBO analysis to support *p*-quinoid resonance forms.³⁰ More recently, Sun et al used electrospray ionization coupled to quadrupole extractive orbitrap (ESI-QE-Orbitrap-MS/MS) in combination with density functional theory (DFT) to establish the thermochemical process and to propose fragmentation pathways for commercial protonated coumarins.³¹ Nevertheless, to date, ESI-MS/MS data concerning 4-aryl-substituted coumarins are scarce.

In this study, we have investigated the fragmentation pathways of a series of synthetic 4-aryl-substituted coumarins by accurate mass electrospray ionization tandem mass spectrometry in combination with thermochemical data estimated by computational chemistry. We have used the thermochemical data to understand the role that the 4-aryl-substituent plays in the formation of diagnostic product ions.

2 | EXPERIMENTAL

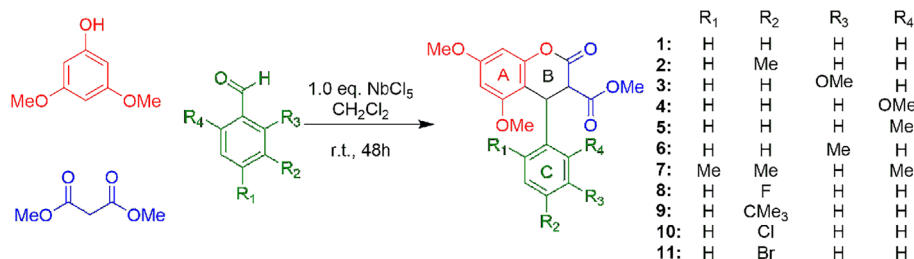
2.1 | Synthesis of 4-aryl-3,4-dihydrocoumarins

The 4-aryl-3,4-dihydrocoumarins **1–11** (designated coumarins **1–11** hereafter; Scheme 1) were obtained by using a previously reported one-pot multicomponent reaction (MCR).^{3,32} Briefly, the general procedure entailed (1) Knoevenagel condensation between a benzaldehyde (1.0 mmol) and dimethylmalonate (132 mg, 1.0 mmol), (2) hydroxylation of the benzylidene formed *in situ* from 3,5-dimethoxyphenol (154 mg, 1.0 mmol), and (3) intramolecular

lactonization. The reaction was catalyzed by niobium pentachloride (NbCl₅, 270 mg, 1.0 mmol) in dichloromethane (2 mL) under nitrogen atmosphere at room temperature for 48 h and quenched with water (3 mL). The organic layer was extracted with dichloromethane (10 mL) and washed with magnesium sulfate. The solvent was removed under reduced pressure, and the crude mixtures were chromatographed through silica gel by using hexane and ethyl acetate (7:3, v/v) as eluent, to give one of the coumarins **1–11** (depending on the starting benzaldehyde) in good yield. All the compounds were analyzed as a mixture of *trans*-enantiomers.

2.2 | Mass spectrometry

Coumarins **1–11** were analyzed on a hybrid quadrupole/time-of-flight MS UltratOF-Q (Bruker Daltonics, USA) fitted with an electrospray ion source operating in the positive ion mode. The samples were dissolved in methanol/water (9:1, v/v) at a concentration of 0.5 mg mL⁻¹ and infused directly into the ionization source by using a Harvard Apparatus system (model 1746, Houston, MA, USA) at a flow rate of 5 μL min⁻¹. Sodium trifluoroacetate (TFA-Na⁺) was employed as an internal standard for calibration. The capillary, cone voltage, puller cone voltage, and RF were set to 2.5 kV, 10.0 V, 3.00 kV, and 0.10 V, respectively. The source temperature and the desolvation temperature were adjusted to 150 and 250°C, respectively. Nitrogen (99.999%) at 7 psi was used as the desolvation (4 L/h), nebulizing (180°C), drying (4 L/h), and collision gas. For the experiments with deuterium exchange, deuterated water (deuterium oxide, D₂O) was added to the coumarin solution, and the [M + D]⁺ ion was selected as the precursor ion. The product ion spectra were obtained by using collision energies ranging from 5 to 50 eV. To establish the fragmentation pathways, *quasi*-MS³ experiments (i.e., fragment ions formed through in-source dissociation) with product ions generated by in-source dissociation were carried out on triple quadrupole MS equipment (QqQ) Xevo TQS (Waters, Milford, MA, USA) equipped with Z-spray and Acquity-H class UPLC system. The sample was dissolved in methanol/water (9:1, v/v) at a concentration of 0.5 mg mL⁻¹ and infused directly into the ESI source by using a Harvard Apparatus system (model 1746, Houston, MA, USA) at a flow rate of 5 μL min⁻¹. The capillary voltage was 3.20 kV, and the extraction cone was set to 50 V to induce in-source dissociation. The gas flow was 700 L/h (0.15 V), and the desolvation temperature was 250°C. Argon (99.999%) was used as the collision gas.



SCHEME 1 Synthesis of 4-aryl-3,4-dihydrocoumarins **1–11**^{3,32}.

2.3 | Computational methods

The structures of coumarins **1–11** were optimized by using the B3LYP/6-31+G(d,p) model in Gaussian 03 suite programs.³³ The model was achieved on the basis of previous studies^{30,34} by considering that errors were very small in comparison to experimental values at a minimum computational cost. All the structures were visualized with the Chemcraft software.³⁵ The stationary point was achieved through the calculation of vibration frequencies employing the same model. To establish the proton affinity (PA) as a descriptor, the enthalpy of the protonation reaction $M + H^+ \rightarrow MH^+$ was evaluated as previously reported in the literature.^{28,36–39} The enthalpy for the proton reaction mentioned above was considered to be $1.48 \text{ kcal mol}^{-1}$.⁴⁰ By employing the same computational model, fragmentation pathways were proposed on the basis of the relative Gibbs energies and relative enthalpies at 298.15 K for coumarins **1–11**. The Gibbs energies were used with caution when the fragmentation pathways were proposed because equilibrium conditions could not be established during the CID experiments.⁴¹

3 | RESULTS AND DISCUSSION

3.1 | Structure–fragmentation relationships

Literature data have shown that structure–fragmentation relationships play a key role in the elucidation of gas-phase fragmentation pathways of compounds that share the same structure core.^{24,25,27,42–44} We obtained structure–fragmentation relationships of protonated coumarins **1–11** by comparing the corresponding product ion spectra at a collision energy (E_{lab}) of 20 eV. We chose this collision energy because it can decrease the relative intensity of the protonated molecule in the product ion spectrum to generate the maximum number of product ions without promoting extensive fragmentation. Plots of the relative intensity (RI, %) versus E_{lab} (eV) from 5 to 50 eV obtained for coumarins **1–11** are provided in the Supporting Information.

Table 1 lists the product ions with relative intensity higher than 3% and their corresponding assignments. The product ion spectra of coumarin **1** obtained at collision energies lower than 10 eV displayed fewer intense product ion than the product ion spectra of coumarins **2–11** (Figure 1). This fact revealed that the presence of substituents at the aromatic ring C of coumarins **2–11** resulted in additional fragmentation pathways and provided other diagnostic product ions as compared to coumarin **1**, which does not bear substituents at ring C, as will be further discussed.

Taking into account that coumarins **1–11** differ in the nature, position, and number of substituents at ring C, a comparative analysis of the product ion spectra of coumarins **1–11** allowed us to identify (1) ions with the same m/z (i.e., the common product ions, formed by eliminations of ring C); (2) ions with different m/z originating from the same fragmentation process that is common to the analyzed series; and (3) ions formed by a diagnostic fragmentation process (i.e., a process that depends on the nature and position of the substituents at ring C).

Product ions **D** (m/z 265), **E** (m/z 221), and **G** (m/z 181) were common product ions of coumarins **1–11** (Scheme 2) and originated from $C_6H_2R_1R_2R_3R_4$, $C_6H_2R_1R_2R_3R_4 + CO_2$, and $C_{10}H_6O_2R_1R_2R_3R_4$ elimination, respectively. On the other hand, methanol (32 Da), $C_4H_4O_3$ (100 Da), $C_8H_{10}O_3$ (154 Da), and $C_9H_8O_3$ or $C_8H_8O_2 + CO_2$ (180 Da) elimination, to produce product ions **B**, **C**, **F**, and **H**, respectively, were common fragmentation processes in coumarins **1–11**. Product ions **J** ($C - C_7H_6O$) and **K** ($J - CH_3OH$) were diagnostic of coumarin **4**, which displays an *ortho*-methoxy group at ring C, whereas product ion **I** ($C - C_4H_8$) was diagnostic of a *tert*-butyl at ring C. Finally, product ion **M** was diagnostic of coumarins **3**, **4**, **8**, **10**, and **11** (Scheme 2).

3.2 | Protonation sites in the gas-phase

Coumarins **1–11** are polyfunctionalized compounds that bear ether (coumarins **3** and **4**) and ester functional groups and halogen atoms (coumarins **8**, **10**, and **11**) that may be susceptible to protonation. Protonation at different sites of the coumarin structure produces different protonated regioisomers (i.e., species that differ only in the position at which the proton is attached), which are referred to in this study as “protomers.”^{46,47} On the basis of gas-phase basicity (GB) and proton affinities (PA), Bouchoux et al reported that the carbonyl oxygen is the most susceptible to protonation in the structure of polyfunctionalized molecules containing carbonyl groups or α,β -unsaturated carbonyl groups.^{48,49} Recently, by using DFT calculations, Sun et al demonstrated that the carbonyl oxygen is the most susceptible to protonation in the coumarin structure.³¹ Here, we estimated PA at the B3LYP/6-31+G(d,p) level of theory. We chose the basis system on the basis of previous studies by our team²⁷ in which this model was shown to produce acceptable results at the smallest computational cost.³⁷ Figure 2 presents the PA estimated by theoretical calculations, which indicated that the methyl ester carbonyl oxygen was the most susceptible to protonation in the structure of coumarins **1–3**, **5–7**, **9**, and **11**. For coumarins **8** and **10**, the δ -lactone carbonyl oxygen gave the highest PA (209.0 and 209.1 kcal mol^{-1} , respectively). In the case of coumarin **4**, which bears the methoxy group at the *ortho* position of ring C, the PA of the oxygen of the methoxy group at the *ortho* position of ring C (220.6 kcal mol^{-1}) was higher than the PA of the ester carbonyl oxygen (213.3 kcal mol^{-1}) and the δ -lactone carbonyl oxygen (216.1 kcal mol^{-1}). The presence of a halogen atom at the *para* position (F, Cl) of coumarins **8** and **10** also decreased the PA of the methyl ester carbonyl oxygen as compared to the lactone carbonyl oxygen. Mason et al described similar effects in their studies on the GB of halogenated toluenes.⁵⁰ The reactivity of aromatic species is governed by qualitative concepts of electronic effects, such as polarization and resonance. Alkyl groups (e.g., methyl groups) can act as electron-releasing groups due to the hyperconjugation effect, whereas halogens act as σ -acceptors and π -donors depending on the nature of the halogen and other substituents in the aromatic ring.^{51,52} In principle, the halogen effect on PA can be associated with a decreasing field effect ($F > Cl > Br$) between the aromatic ring containing the halogen at the *para* position and the ester

TABLE 1 Product ions of protonated 4-aryl-3,4-dihydrocoumarins **1–11** at a collision energy of 20 eV.

	Assignment	Calculated m/z	Experimental m/z	RI	Error (ppm) ^a	Ion formula
1	A ([M + H] ⁺)	343.1176	343.1182	15	−1.7	C ₁₉ H ₁₉ O ₆ ⁺
	B (A-MeOH)	311.0914	311.0925	8	−3.5	C ₁₈ H ₁₅ O ₅ ⁺
	C (A-C ₄ H ₄ O ₃)	243.1016	243.1016	100	0.0	C ₁₅ H ₁₅ O ₃ ⁺
	D (A-C ₆ H ₆)	265.0707	265.0712	22	−1.9	C ₁₃ H ₁₃ O ₆ ⁺
	E (D-CO ₂)	221.0808	221.0813	31	−2.3	C ₁₂ H ₁₃ O ₄ ⁺
	F (A-C ₈ H ₁₀ O ₃)	189.0546	189.0544	12	1.1	C ₁₁ H ₉ O ₃ ⁺
	G (A-C ₁₀ H ₁₀ O ₂)	181.0495	181.0498	54	−1.7	C ₉ H ₉ O ₄ ⁺
	H (B-C ₈ H ₈ O ₂ -CO ₂)	131.0491	131.0486	5	3.8	C ₉ H ₇ O ⁺
	L (C-C ₈ H ₈ O ₃)	91.0542	91.0546	<3	−4.4	C ₇ H ₇ ⁺
2	A ([M + H] ⁺)	357.1333	357.1327	18	1.7	C ₂₀ H ₂₁ O ₆ ⁺
	B (A-MeOH)	325.1071	325.1076	10	−1.5	C ₁₉ H ₁₇ O ₅ ⁺
	C (A-C ₄ H ₄ O ₃)	257.1172	257.1176	100	−1.6	C ₁₆ H ₁₇ O ₃ ⁺
	D (A-C ₇ H ₈)	265.0707	265.0698	21	3.4	C ₁₃ H ₁₃ O ₆ ⁺
	E (D-CO ₂)	221.0808	221.0801	37	3.2	C ₁₂ H ₁₃ O ₄ ⁺
	F (A-C ₈ H ₁₀ O ₃)	203.0703	203.0708	18	−2.5	C ₁₂ H ₁₁ O ₃ ⁺
	G (A-C ₁₁ H ₁₂ O ₂)	181.0495	181.0485	55	5.5	C ₉ H ₉ O ₄ ⁺
	H (B-C ₈ H ₈ O ₂ -CO ₂)	145.0648	145.0643	17	3.4	C ₁₀ H ₉ O ⁺
	L (C-C ₈ H ₈ O ₃)	105.0699	105.0697	7	3.8	C ₈ H ₉ ⁺
3	A ([M + H] ⁺)	373.1282	373.1285	12	−0.8	C ₂₀ H ₂₁ O ₇ ⁺
	B (A-MeOH)	341.1020	341.1028	7	−2.3	C ₁₉ H ₁₇ O ₆ ⁺
	C (A-C ₄ H ₄ O ₃)	273.1121	273.1123	100	−0.7	C ₁₆ H ₁₇ O ₄ ⁺
	D (A-C ₇ H ₈ O)	265.0707	265.0707	26	−3.8	C ₁₃ H ₁₃ O ₆ ⁺
	E (D-CO ₂)	221.0808	221.0808	40	−2.3	C ₁₂ H ₁₃ O ₄ ⁺
	F (A-C ₈ H ₁₀ O ₃)	219.0652	219.0652	17	−2.7	C ₁₂ H ₁₁ O ₄ ⁺
	G (A-C ₁₁ H ₁₂ O ₃)	181.0495	181.0495	59	−1.7	C ₉ H ₉ O ₄ ⁺
	H (B-C ₈ H ₈ O ₂ -CO ₂)	161.0597	161.0597	15	−1.2	C ₁₀ H ₉ O ₂ ⁺
	L (C-C ₈ H ₈ O ₃)	121.0648	121.0645	3	2.5	C ₈ H ₉ O ⁺
4	A ([M + H] ⁺)	373.1282	373.1291	11	−2.4	C ₂₀ H ₂₁ O ₇ ⁺
	B (A-MeOH)	341.1020	341.1025	19	−1.5	C ₁₉ H ₁₇ O ₆ ⁺
	C (A-C ₄ H ₄ O ₃)	273.1121	273.1122	100	−0.4	C ₁₆ H ₁₇ O ₄ ⁺
	D (A-C ₇ H ₈ O)	265.0707	265.0704	35	1.1	C ₁₃ H ₁₃ O ₆ ⁺
	E (D-CO ₂)	221.0808	221.0801	45	3.2	C ₁₂ H ₁₃ O ₄ ⁺
	F (A-C ₈ H ₁₀ O ₃)	219.0652	219.0657	38	−2.3	C ₁₂ H ₁₁ O ₄ ⁺
	G (A-C ₁₁ H ₁₂ O ₃)	181.0495	181.0490	57	2.8	C ₉ H ₉ O ₄ ⁺
	J (C-CH ₂ O-C ₆ H ₄)	167.0703	167.0707	9	−2.4	C ₉ H ₁₁ O ₃ ⁺
	H (B-C ₈ H ₈ O ₂ -CO ₂)	161.0597	161.0592	16	3.1	C ₁₀ H ₉ O ₂ ⁺
	K (J-MeOH)	135.0441	135.0445	5	−3.0	C ₈ H ₇ O ₂ ⁺
	L (C-C ₈ H ₈ O ₃)	121.0648	121.0652	11	−3.3	C ₈ H ₉ O ⁺
	5	A ([M + H] ⁺)	357.1333	357.1323	12	2.8
B (A-MeOH)		325.1071	325.1068	9	0.9	C ₁₉ H ₁₇ O ₅ ⁺
C (A-C ₄ H ₄ O ₃)		257.1172	257.1169	100	1.2	C ₁₆ H ₁₇ O ₃ ⁺
D (A-C ₇ H ₈)		265.0707	265.0699	17	3.0	C ₁₃ H ₁₃ O ₆ ⁺
E (D-CO ₂)		221.0808	221.0803	38	2.3	C ₁₂ H ₁₃ O ₄ ⁺
F (A-C ₈ H ₁₀ O ₃)		203.0703	203.0699	25	2.0	C ₁₂ H ₁₁ O ₃ ⁺
G (A-C ₁₁ H ₁₂ O ₂)		181.0495	181.0491	43	2.2	C ₉ H ₉ O ₄ ⁺
H (C ₈ H ₈ O ₂ -CO ₂)		145.0648	145.0645	10	2.1	C ₁₀ H ₉ O ⁺
L (C-C ₈ H ₈ O ₃)		105.0699	105.0695	6	3.8	C ₈ H ₉ ⁺

TABLE 1 (Continued)

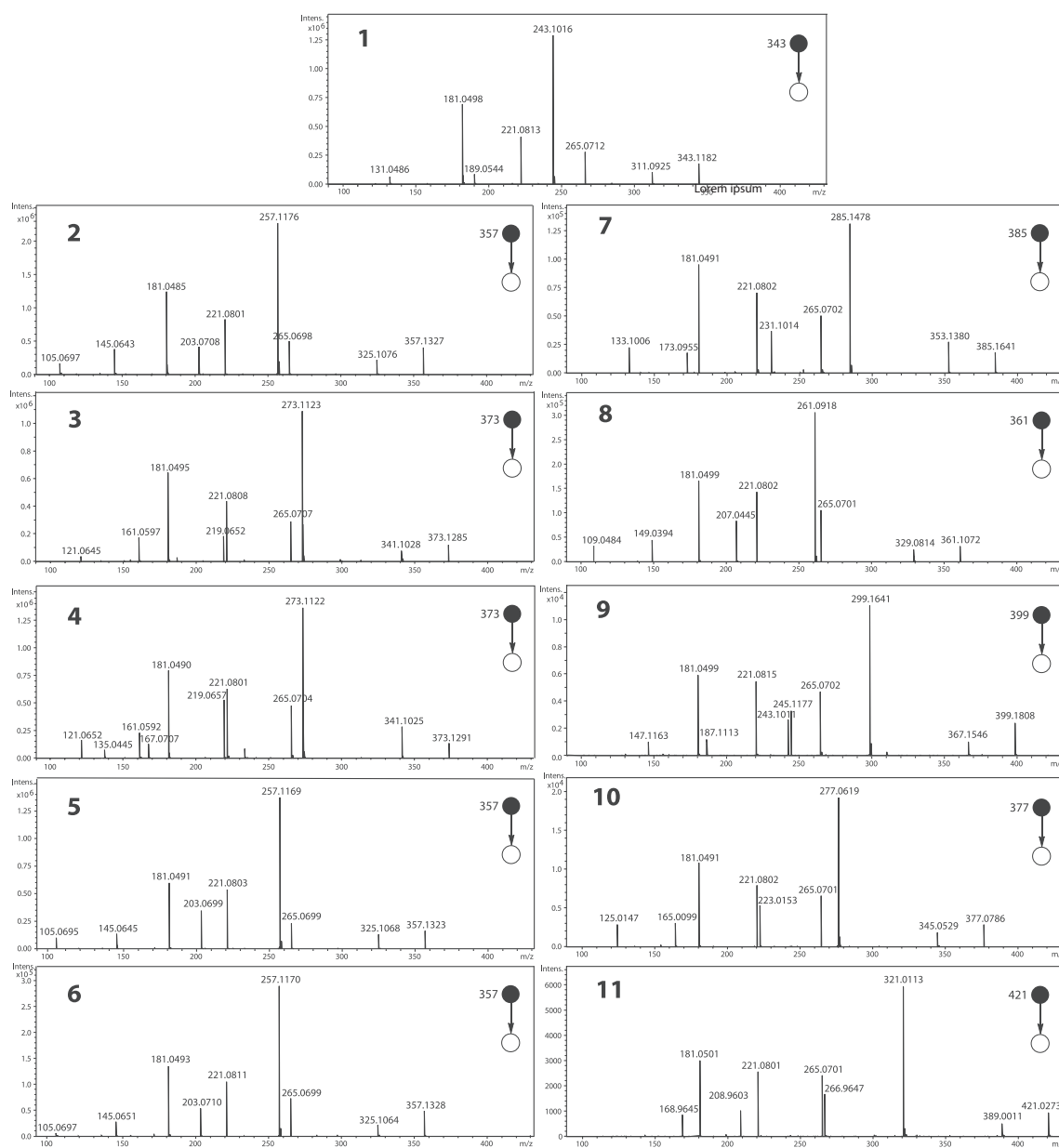
	Assignment	Calculated m/z	Experimental m/z	RI	Error (ppm) ^a	Ion formula
6	A ([M + H] ⁺)	357.1333	357.1328	17	1.4	C ₂₀ H ₂₁ O ₆ ⁺
	B (A-MeOH)	325.1071	325.1064	7	2.2	C ₁₉ H ₁₇ O ₅ ⁺
	C (A-C ₄ H ₄ O ₃)	257.1172	257.1170	100	0.8	C ₁₆ H ₁₇ O ₃ ⁺
	D (A-C ₇ H ₈)	265.0707	265.0699	25	3.0	C ₁₃ H ₁₃ O ₆ ⁺
	E (D-CO ₂)	221.0808	221.0811	36	-1.4	C ₁₂ H ₁₃ O ₄ ⁺
	F (A-C ₈ H ₁₀ O ₃)	203.0703	203.0710	19	-3.4	C ₁₂ H ₁₁ O ₃ ⁺
	G (A-C ₁₁ H ₁₂ O ₂)	181.0495	181.0493	45	1.1	C ₉ H ₉ O ₄ ⁺
	H (C ₈ H ₈ O ₂ -CO ₂)	145.0648	145.0651	8	-2.1	C ₁₀ H ₉ O ⁺
	L (C-C ₈ H ₈ O ₃)	105.0699	105.0697	<3	4.8	C ₈ H ₉ ⁺
7	A ([M + H] ⁺)	385.1646	385.1641	14	1.3	C ₂₂ H ₂₅ O ₆ ⁺
	B (A-MeOH)	353.1384	353.1380	21	1.1	C ₂₁ H ₂₁ O ₅ ⁺
	C (A-C ₄ H ₄ O ₃)	285.1485	285.1478	100	2.5	C ₁₈ H ₂₁ O ₃ ⁺
	D (A-C ₉ H ₁₂)	265.0707	265.0702	38	1.9	C ₁₃ H ₁₃ O ₆ ⁺
	E (D-CO ₂)	221.0808	221.0802	54	2.7	C ₁₂ H ₁₃ O ₄ ⁺
	F (A-C ₈ H ₁₀ O ₃)	231.1016	231.1014	29	0.9	C ₁₄ H ₁₅ O ₃ ⁺
	G (A-C ₁₃ H ₆ O ₂)	181.0495	181.0491	74	2.2	C ₉ H ₉ O ₄ ⁺
	H (B-C ₈ H ₈ O ₂ -CO ₂)	173.0961	173.0955	14	3.5	C ₁₂ H ₁₃ O ⁺
	L (C-C ₈ H ₈ O ₃)	133.1012	133.1006	18	4.5	C ₁₀ H ₁₃ ⁺
8	A ([M + H] ⁺)	361.1082	361.1072	11	2.8	C ₁₉ H ₁₈ FO ₆ ⁺
	B (A-MeOH)	329.0820	329.0814	9	1.8	C ₁₈ H ₁₄ FO ₅ ⁺
	C (A-C ₄ H ₄ O ₃)	261.0921	261.0918	100	1.1	C ₁₅ H ₁₄ FO ₃ ⁺
	D (A-C ₆ H ₅ F)	265.0707	265.0701	35	2.3	C ₁₃ H ₁₃ O ₆ ⁺
	E (D-CO ₂)	221.0808	221.0802	47	2.7	C ₁₂ H ₁₃ O ₄ ⁺
	F (A-C ₈ H ₁₀ O ₃)	207.0452	207.0445	28	3.4	C ₁₁ H ₈ FO ₃ ⁺
	G (A-C ₁₀ H ₉ FO ₂)	181.0495	181.0499	55	-2.2	C ₉ H ₉ O ₄ ⁺
	H (B-C ₈ H ₈ O ₂ -CO ₂)	149.0397	149.0394	15	2.0	C ₉ H ₆ FO ⁺
	L (C-C ₈ H ₈ O ₃)	109.0488	109.0484	12	3.7	C ₇ H ₆ F ⁺
9	A ([M + H] ⁺)	399.1802	399.1808	20	-1.5	C ₂₃ H ₂₇ O ₆ ⁺
	B (A-MeOH)	367.1540	367.1546	8	-1.6	C ₂₂ H ₂₃ O ₅ ⁺
	C (A-C ₄ H ₄ O ₃)	299.1642	299.1641	100	0.3	C ₁₉ H ₂₃ O ₃ ⁺
	D (A-C ₁₀ H ₁₄)	265.0707	265.0702	43	1.9	C ₁₃ H ₁₃ O ₆ ⁺
	I (C-C ₄ H ₈)	243.1016	243.1011	24	2.1	C ₁₅ H ₁₅ O ₃ ⁺
	E (D-CO ₂)	221.0808	221.0815	50	-3.2	C ₁₂ H ₁₃ O ₄ ⁺
	F (A-C ₈ H ₁₀ O ₃)	245.1172	245.1177	27	-2.0	C ₁₅ H ₁₇ O ₃ ⁺
	G (A-C ₁₄ H ₁₈ O ₂)	181.0495	181.0499	53	-2.2	C ₉ H ₉ O ₄ ⁺
	H (B-C ₈ H ₈ O ₂ -CO ₂)	187.1117	187.1113	11	2.1	C ₁₃ H ₁₅ O ⁺
	L (C-C ₈ H ₈ O ₃)	147.1168	147.1163	9	3.4	C ₁₁ H ₁₅ ⁺
	10	A ([M + H] ⁺)	377.0786	377.0786	15	1.1
B (A-MeOH)		345.0524	345.0529	10	-1.4	C ₁₈ H ₁₄ ClO ₅ ⁺
C (A-C ₄ H ₄ O ₃)		277.0626	277.0619	100	2.5	C ₁₅ H ₁₄ ClO ₃ ⁺
D (A-C ₆ H ₅ Cl)		265.0707	265.0701	36	2.3	C ₁₃ H ₁₃ O ₆ ⁺
E (D-CO ₂)		221.0808	221.0802	41	2.7	C ₁₂ H ₁₃ O ₄ ⁺
F (A-C ₈ H ₁₀ O ₃)		223.0156	223.0153	28	1.3	C ₁₁ H ₈ ClO ₃ ⁺
G (A-C ₁₀ H ₉ ClO ₂)		181.0495	181.0491	56	2.2	C ₉ H ₉ O ₄ ⁺
H (B-C ₈ H ₈ O ₂ -CO ₂)		165.0102	165.0099	16	1.8	C ₉ H ₆ ClO ⁺
L (C-C ₈ H ₈ O ₃)		125.0153	125.0147	15	4.8	C ₇ H ₆ Cl ⁺

(Continues)

TABLE 1 (Continued)

	Assignment	Calculated m/z	Experimental m/z	RI	Error (ppm) ^a	Ion formula
11	A ($[M + H]^+$)	421.0281	421.0273	15	1.9	$C_{19}H_{18}BrO_6^+$
	B (A-MeOH)	389.0019	389.0011	7	2.1	$C_{18}H_{14}BrO_5^+$
	C (A- $C_4H_4O_3$)	321.0121	321.0113	100	2.5	$C_{15}H_{14}BrO_3^+$
	D (A- C_6H_5Br)	265.0707	265.0701	41	2.3	$C_{13}H_{13}O_6^+$
	E (D- CO_2)	221.0808	221.0801	43	3.2	$C_{12}H_{13}O_4^+$
	F (A- $C_8H_{10}O_3$)	266.9651	266.9647	27	1.5	$C_{11}H_8BrO_3^+$
	G (A- $C_{10}H_9BrO_2$)	181.0495	181.0501	50	-3.3	$C_9H_9O_4^+$
	H (B- $C_8H_8O_2-CO_2$)	208.9597	208.9603	17	-2.9	$C_9H_6BrO^+$
	L (C- $C_8H_8O_3$)	168.9647	168.9645	13	1.2	$C_7H_6Br^+$

Abbreviation: RI, relative intensity (%).

^aCalculated according to the formula $10^6 \times (m_{\text{calculated}} - m_{\text{experimental}}/m_{\text{experimental}})$.⁴⁵FIGURE 1 Product ion spectra of protonated 4-aryl-3,4-dihydrocoumarins 1-11 (N_2 , E_{lab} of 20 eV).

SCHEME 2 Structure-fragmentation relationships of protonated 4-aryl-3,4-dihydrocoumarins **1–11**.

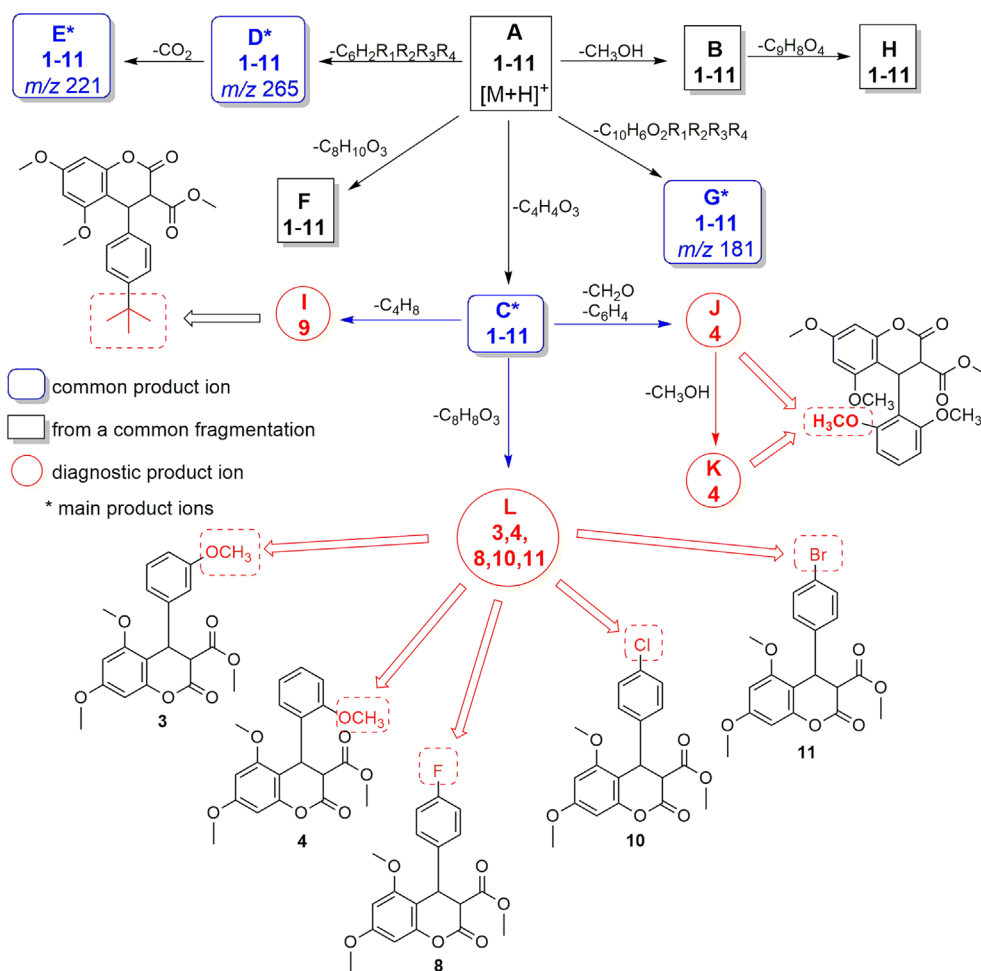
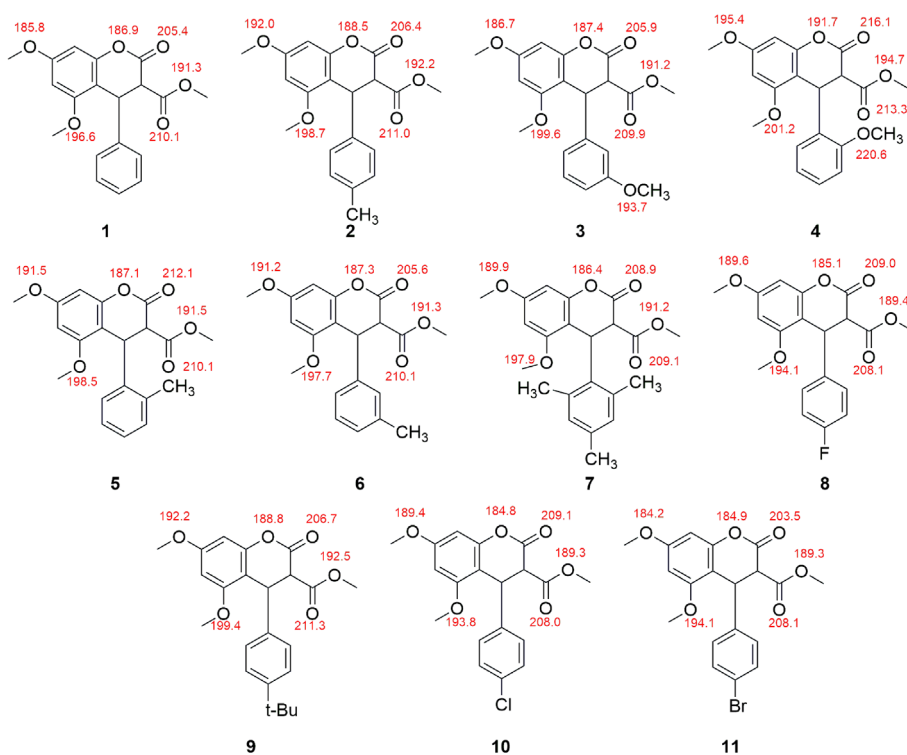


FIGURE 2 Proton affinities (PA) for 3-aryl-3,4-dihydrocoumarins **1–11**, calculated at the B3LYP/6-31+G(d,p) level. The PA are in kcal.mol⁻¹.



carbonyl oxygen.^{53,54} As for coumarin **7**, the presence of methyl groups at positions 2 and 6 (i.e., at *ortho* positions) might affect the ring C orientation relative to rings A and B and the ester carbonyl group. However, a deeper understanding of the substituent effects requires that more compounds containing a wider diversity of substituents at different positions of ring C to be analyzed.

Although it is well established that the PA and GB values are important parameters to identify the most stable protomer, there has been an extensive discussion on the protomer that triggers the fragmentation processes under collision-induced dissociation (CID) conditions. In principle, three major possibilities could be considered: (1) the proton remains attached to the most basic site of the structure, even after CID, so that CID increases the internal energy content of the most stable protomer and triggers the fragmentation processes⁵⁵; (2) the proton is initially attached to the most basic site of the molecule, but it can migrate to other less basic sites under CID conditions to trigger fragmentation – this is known as the “mobile proton model”⁵⁶; (3) protonation can occur at different sites, producing a population of all the possible protomers, with an excess of the most stable protomer population—in this case, the most labile protomer triggers the fragmentation processes.⁴⁴ Recently, Reis et al brought a new light to the “most stable protomer” versus “more labile protomer” discussion.⁵⁷ The authors performed PM7 calculations and elaborated potential energy surface diagrams to elucidate the fragmentation of several illustrative selected molecules to conclude that an equilibrium of protomers may be attained before fragmentation.⁵⁷ In this study, data from the deuterium exchange experiments indicated that most (but not all) product ions of protonated **1–11** were formed from labile protomers. Indeed, the formation of some product ions (e.g., **B**, **C**, and **D**) requires the proton/deuterium to be attached in different basic sites in the structures of compounds **1–11**, as it will be further discussed. Therefore, even though the PA and GB values provide important guidance to identify the thermodynamically most favored protomers, kinetically controlled protonation can also take place in less favored sites (e.g., due to steric factors),⁵⁸ which makes feasible the coexistence of different protomers in the gas phase. These results follow the “pre-fragmentation equilibrium of protomers” concept proposed by Reis et al.⁵⁷

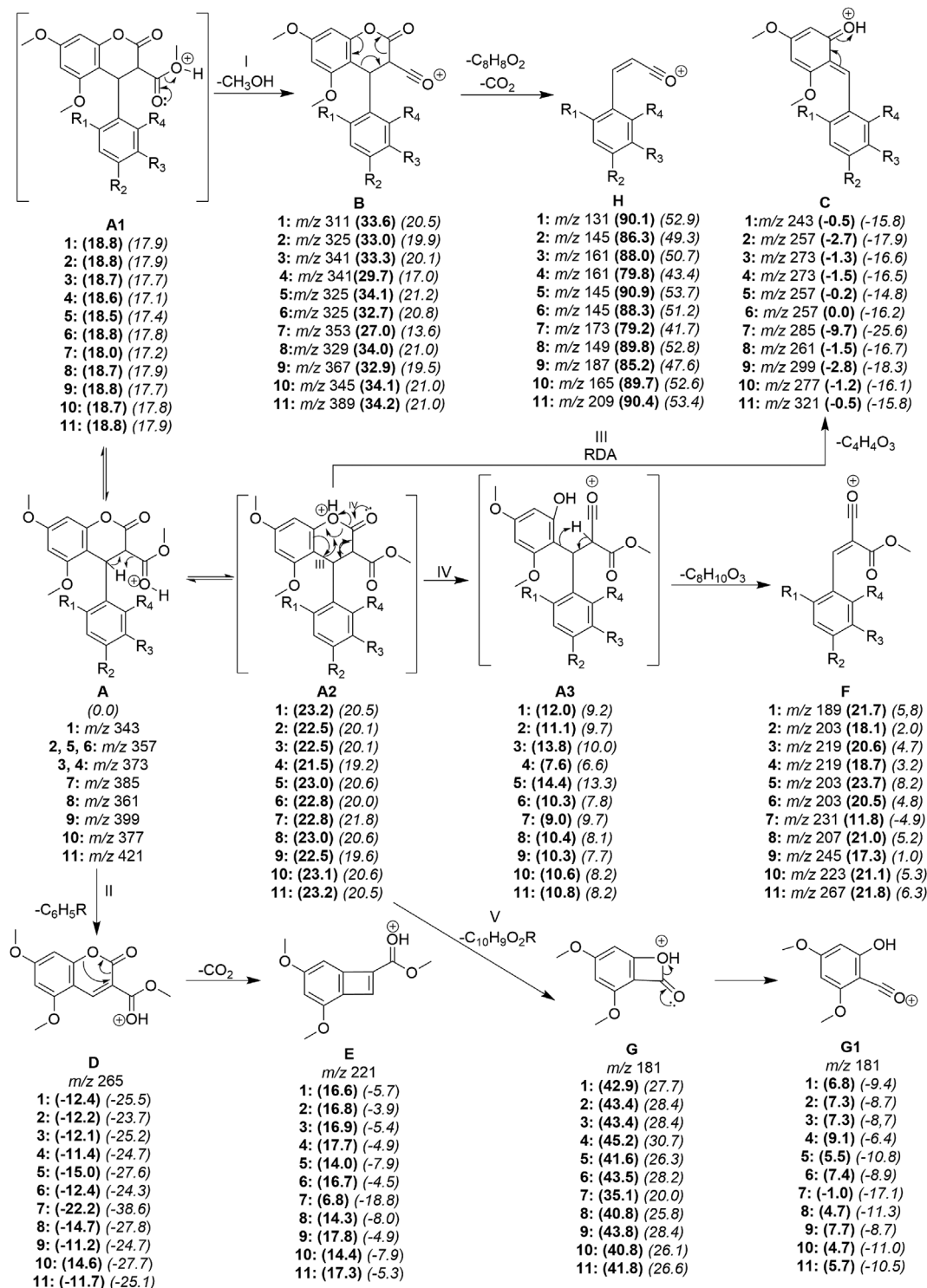
When it comes to coumarin **4**, a proton might migrate spontaneously from the methyl ether oxygen (PA = 220.6 kcal mol⁻¹)—the labile protomer **A1** (Scheme 3)—to the methyl ester carbonyl oxygen (PA = 213.3 kcal mol⁻¹) during geometry optimization to produce **A**, which is the most stable protomer in the equilibrium with **A1** and **A2** (Scheme 3). This proton migration is facilitated by the spatial proximity between the *ortho*-methoxy group oxygen and the ester carbonyl oxygen. Demarque et al reported that protons can migrate during time-scaling experiments depending on kinetic and thermodynamic factors.³⁹ Previous studies have demonstrated that proton migrations during computational optimizations can trigger important fragmentation reactions.^{59,60} On the other hand, the most labile protomers **A1** and **A2** can fragment to produce **B**, **C**, and **D**, which arises most of the product ions of compounds **1–11** (Scheme 3), as will be further discussed in this work.

3.3 | Common fragmentation processes and formation of common product ions of coumarins **1–11**

Product ion **B** resulted from methanol elimination from the protomer **A1** (pathway I; Scheme 3). In principle, this elimination can occur through two mechanisms: (1) remote hydrogen rearrangement involving the α -carbonyl hydrogen, to form a ketene,^{25,42} and (2) charge-induced fragmentation, triggered by proton migration to the ester oxygen, to produce an acylium ion (pathway I; Scheme 3).⁴² Data from deuterium exchange experiments indicated that CH₃OD was eliminated, implying that charge-induced fragmentation was involved in product ion **B** formation (see Supporting Information). Proton migration from the most basic site (methyl ester carbonyl oxygen in coumarins **1–3**, **5–7**, **9**, and **11**; δ -lactone carbonyl oxygen in coumarins **8** and **10**; or the methyl ether in **4**) to the methyl ester oxygen (a less basic site) is in accordance with the proton mobile theory.^{61–63} This migration and the consequent equilibrium between the different protomers is feasible when the energy transferred to the center-of-mass (E_{com}) of the precursor ion upon the CID process is higher than the difference between the ΔH of the two protonated species. At E_{lab} of 20 eV, the E_{com} ($E_{com} = E_{lab} [m_c/(m_c + m_i)]$)^{41,55} of **1** (m/z 343), **2** (m/z 357), **3** (m/z 373), **4** (m/z 373), **5** (m/z 357), **6** (m/z 357), **7** (m/z 385), **8** (m/z 361), **9** (m/z 399), **10** (m/z 377), and **11** (m/z 411) was calculated to be 34.7, 33.5, 32.1, 32.1, 33.5, 33.5, 31.2, 33.1, 30.2, 31.8, and 28.7 kcal mol⁻¹, respectively, which was consistent with the aforementioned proton migration. Product ion **H** originated from product ion **B** through retro-Diels–Alder (RDA) reaction⁶⁴ at ring B, an endothermic (ΔH between 50.1 and 56.8 kcal mol⁻¹) and endergonic (ΔG between 26.4 and 32.5 kcal mol⁻¹) process.

Direct ring C elimination from the most stable protomer **A** through remote hydrogen rearrangement³⁹ to produce product ion **D** (m/z 265) (pathway II; Scheme 3) was exothermic (ΔH between –11.2 and –22.2 kcal mol⁻¹) and exergonic (ΔG between –38.6 and –23.7 kcal mol⁻¹). At collision energies of 5 and 10 eV, the product ion **D** was one of the most intense in the product ion spectra of coumarins **1–11** (see break down graphs in the Supporting Information). However, at higher collision energies, (1) product ions **D** can be converted into **E** through δ -lactone ring contraction and the consequent CO₂ elimination^{39,65} through an endothermic (ΔH between 29.0 and 29.1 kcal mol⁻¹) and endergonic (ΔG between 19.7 and 19.8 kcal mol⁻¹) process (Scheme 3); (2) the population of the less stable protomer **A2** increased compared to **A** because a proton migrated from the ester carbonyl oxygen to the δ -lactone ring oxygen heteroatom. Thus, the product ion **C** (pathway III; Scheme 3) emerged as the base peak in the product ion spectra at collision energies higher than 20 eV (see break down graphs in the Supporting Information).

Product ions **C** (pathway III), **F** (pathway IV), and **G** (pathway V) originated from the same protomer **A2**, a protomer of **A** resulting from proton migration from the carbonyl oxygen to the δ -lactone ring oxygen heteroatom (Scheme 3). ΔH (between 21.5 and 23.2 kcal mol⁻¹) and ΔG (between 19.2 and 21.2 kcal mol⁻¹) estimated for this proton migration revealed that **A** \rightarrow **A2** conversion was feasible under CID conditions. Formation of the highly conjugated oxonium ion **C** from



SCHEME 3 Formation of the common product ions A-H of 3,4-dihydro-4-arylcoumarins 1-11. The enthalpies and Gibbs energies calculated at the B3LYP/6-31+G(d,p) level are in kcal.mol⁻¹.

protomer A2 (pathway III; Scheme 3) involved C₄H₄O₃ (100 Da) elimination through an RDA at ring B, resembling what has been reported for flavonoids.⁶⁶ On the other hand, product ion G formation from protomer A2 (pathway V; Scheme 3) involved δ-lactone ring contraction, to produce a β-lactone ring, whereas the resonance-stabilized

acylium ion F (pathway IV; Scheme 3) emerged after protomer A2 was converted to acylium ion A3. Negative ΔH (between -32.5 and -22.7 kcal mol⁻¹) and ΔG (between -47.4 and -35.4 kcal mol⁻¹) for product ion C formation from protomer A2 were lower as compared to product ion G formation from protomer A2 (ΔH between 7.2 and

14.3 kcal mol⁻¹; ΔG between 8.0 and 14.9 kcal mol⁻¹). Although lower ΔH (between -13.9 and -8.6 kcal mol⁻¹) and ΔG (between -7.3 and -12.6 kcal mol⁻¹) were estimated for the conversion of protomer **A2** to acylium ion **A3** (pathway IV; Scheme 3) compared to product ion **C** formation from protomer **A2**, product ion **F** formation from acylium ion **A3** was an energetically less favored process (ΔH between -8.6 and 13.9 kcal mol⁻¹; ΔG between -7.3 and -12.6 kcal mol⁻¹) than product ions **C** formation from **A2** (ΔH values between -32.5 and -22.8 kcal mol⁻¹; ΔG between -47.4 and -35.4 kcal mol⁻¹). This could be the reason why product ion **C** was more intense than product ions **B**, **D**, **E**, **F**, **G**, and **H** at $E_{lab} = 20$ eV. Nevertheless, at E_{lab} higher than 40 eV, product ion **G** became the base peak in the product ion spectra of coumarins **1-11** (see plots in the Supporting Information).

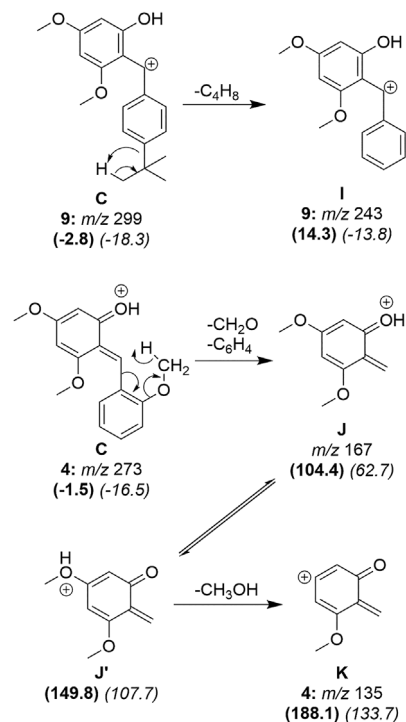
3.4 | Formation of diagnostic product ions

Although the product ion spectra of coumarins **1-11** shared the most intense product ions, the nature of the substituents at ring C played an interesting role in the formation of some diagnostic ions. The relative intensity of these diagnostic ions was low (about 5% or lower) at $E_{lab} = 20$ eV, but the ions intensified with increasing collision energies (see breakdown graphs in the Supporting Information). However, because the formation of these ions was associated with the nature, position, and electronic effect of the substituents at ring C, they will be also discussed here.

The presence of a *tert*-butyl group in ring C of coumarin **9** was associated with formation of product ion **I** (m/z 243) through isobutene (C₄H₈) elimination from product ion **C** through remote hydrogen rearrangement⁶⁶ (Scheme 4). The calculated ΔH and ΔG were 17.1 and 4.5 kcal mol⁻¹, respectively. Isobutene (56 Da) elimination has also been reported for prenylated compounds,⁶⁷ so it cannot be considered specific for a *tert*-butyl group.

The product ion **J** emerged only in the product ion spectrum of coumarin **4**, which bears an *ortho*-methoxy group at ring C. The absence of product ion **J** in the product ion spectrum of coumarin **3**, which is a regioisomer of coumarin **4**, evidenced that product ion **J** formation depended on the methoxy group at the *ortho* position. Indeed, the concerted and simultaneous elimination of formaldehyde (CH₂O, 30 Da) and benzyne (C₆H₄, 76 Da) cannot occur in the case of coumarin **3**, which has a *meta*-methoxy group (Scheme 4). Nevertheless, ΔH and ΔG that were estimated to be necessary for product ion **C** to be converted to product ion **J** (105.9 and 79.2 kcal mol⁻¹) and then for product ion **J** to be converted to aryl ion **K** (83.7 and 26.0 kcal mol⁻¹, respectively) were relatively high, which accounted for the low relative intensity of the product ions **J** and **K** in the product ion spectrum of coumarin **4** at $E_{lab} = 20$ eV.

Product ion **L** formation from **C** involves the conversion of a secondary benzylic carbocation to a primary benzylic carbocation, followed by rearrangement to an aromatic tropylium ion **L1**,⁶⁸ as shown in Scheme 5. Justino et al have proposed similar mechanisms



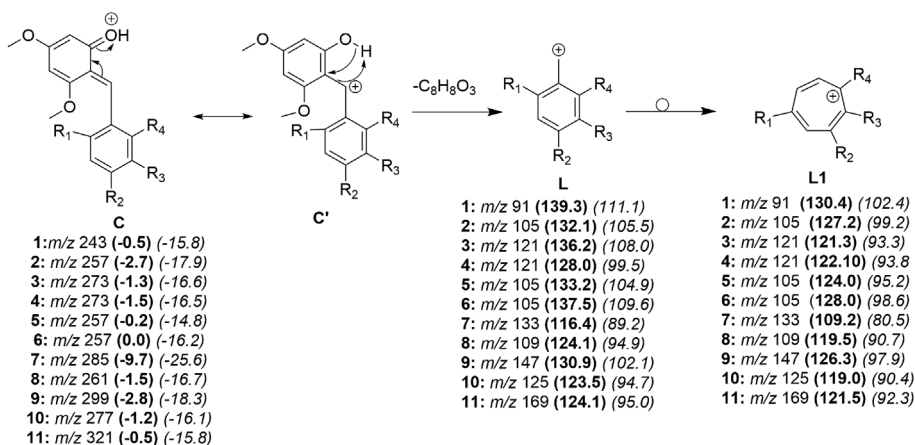
SCHEME 4 Formation of the diagnostic product ions **I**, **J**, and **K**. The enthalpies and Gibbs energies calculated at the B3LYP/6-31+G (d,p) level are in kcal mol⁻¹.

and structures for flavone and flavonol aglycones.⁶⁶ This ion can be useful to identify the nature of the substituents at ring C.

Although the **C** → **L** conversion should be highly endergonic and endothermic for coumarins **1-11** (ΔH between 123.6 and 137.5 kcal mol⁻¹; ΔG between 110.8 and 124.6 kcal mol⁻¹), the relative intensity of the product ion **L** in the product ion spectrum of coumarins **2-11** obtained at $E_{lab} = 20$ eV should vary according to the nature and position of the substituents at ring C. In the case of coumarin **1**, without a substituent at ring C, product ion **L** (m/z 91) did not emerge in its product ion spectrum. These differences could be associated with the different abilities of the substituents at ring C to stabilize the structure of product ion **L** or its corresponding tropylium ion **L1** (Scheme 5).

Thermochemical data, estimated at the B3LYP level of theory, revealed that coumarins **8**, **10**, and **11**, which bear a halogen at the *para* position of ring C, required the lowest ΔH and ΔG to form product ion **L** from product ion **C** (125.6 and 111.6 kcal mol⁻¹, 124.7 and 110.8 kcal mol⁻¹, and 124.6 and 110.8 kcal mol⁻¹, respectively). Indeed, halogens (F for coumarin **8**, Cl for coumarin **10**, and Br for coumarin **11**) can stabilize the benzylic carbocation **L** and the corresponding tropylium ion **L1** due to their electron-releasing mesomeric effect. Product ion **L** could also be stabilized by the methoxy group at the *ortho* position of coumarin **4** ($\Delta H = 129.5$ kcal mol⁻¹, $\Delta G = 116.0$ kcal mol⁻¹). On the other hand, for coumarin **3**, its higher ΔH and ΔG (137.5 and 124.6 kcal mol⁻¹, respectively) as compared to coumarin

SCHEME 5 Formation of the diagnostic product ion **M**. The enthalpies and Gibbs energies calculated at the B3LYP/6-31+G(d,p) level are in kcal mol⁻¹.



4 corroborated that the methoxy group at the *meta* position of ring C cannot stabilize product ion **L** as effectively as the methoxy group at the *ortho* position.

Comparison of ΔH and ΔG of coumarins **5**, **6**, and **2**, which display a methyl group at the *ortho*, *meta*, and *para* positions of ring C, respectively, indicated that product ion **L** stabilization depended on the methyl group position. ΔH and ΔG calculated for coumarin **6** (a methyl group at the *meta* position) to produce product ion **L** from product ion **C** (137.5 and 125.8 kcal mol⁻¹, respectively) were higher compared to coumarin **5** (a methyl group at the *ortho* position, 133.4 and 119.7 kcal mol⁻¹, respectively) and **2** (a methyl group at the *para* position, 134.8 and 123.4 kcal mol⁻¹, respectively). This result revealed that product ion **L** stabilization promoted by the electron-releasing methyl group at the *meta* position was less effective compared to the coumarins where the same group is at the *ortho* or *para* position. Thermochemical data also indicated that stabilization of the *tert*-butyl group at the *para* position resembled stabilization of the methyl group at the same position. Furthermore, the electron-releasing effect of the methyl groups on product ion **L** stabilization was additive, as corroborated by the lower ΔH (126.1 kcal mol⁻¹) and ΔG (114.8 kcal mol⁻¹) calculated for coumarin **7** as compared to coumarins **2**, **5**, and **6**.

4 | CONCLUSIONS

Protonated 4-aryl-3,4-dihydrocoumarins **1–11** have similar gas-phase fragmentation pathways. Most product ions originate from C₈H₈O₂, CO₂, C₄H₄O₃, C₈H₁₀O₃, or CH₃OH elimination through RDA reactions, remote hydrogen rearrangements (β -eliminations), and β -lactone ring contraction. However, formation of the benzylic product ion **L** and its corresponding tropylium ion **L1** is diagnostic of the substituents at ring C. The estimated thermochemical data revealed that the most abundant product ions involve lower ΔH and ΔG and demonstrated that the nature and the position of the substituents at ring C play a key role in the formation of **L** and determine its relative intensity in the product ion spectrum. The results of this study contribute to knowledge of the gas-phase ion chemistry of this important class

of organic compounds and provide a convenient means to identify the substituent at ring C in metabolism studies of compounds **1–11** via LC-ESI-MS/MS analyses.

AUTHOR CONTRIBUTIONS

Herbert J. Dias analyzed all the MS data, proposed the fragmentation pathways, and run the theoretical calculations; William H. Santos synthesized the coumarins **1–11**; Luis C. S. Filho supervised the synthesis. Eduardo J. Crevelin ran all the MS experiments; J. Scott McIndoe read critically and corrected the draft; Ricardo Vessecchi supervised the theoretical calculations; Antônio E. M. Crotti designed the work and drafted and edited the manuscript. All the authors have read the final manuscript and approved its submission.

ACKNOWLEDGMENTS

The authors thank the São Paulo Research Foundation (FAPESP, grant nos. 13/20094-0 and 16/03036-4) for financial support and to National Council for Scientific and Technological Development (CNPq, proc. 310648/2022-0) for fellowships. The authors also thank José Carlos Tomaz for the ESI-TOF-MS/MS analyses.

CONFLICT OF INTEREST STATEMENT

The authors declare that there is no conflict of interest regarding financial, ethical, and human and animal rights. All procedures for experiments followed were in accordance with the ethical standard.

DATA AVAILABILITY STATEMENT

The data that support the findings of this study are openly available in ChemRxiv at <https://chemrxiv.org/>, reference number 10.26434/chemrxiv-2024-l3wwz.

ORCID

Herbert J. Dias <https://orcid.org/0000-0001-6612-2295>

Luis C. S. Filho <https://orcid.org/0000-0001-6674-2160>

Eduardo J. Crevelin <https://orcid.org/0000-0001-8708-147X>

J. Scott McIndoe <https://orcid.org/0000-0001-7073-5246>

Ricardo Vessecchi <https://orcid.org/0000-0001-8472-3190>

Antônio E. M. Crotti <https://orcid.org/0000-0002-1730-1729>

REFERENCES

- Lončarić M, Gašo-Sokač D, Jokić S, Molnar M. Recent advances in the synthesis of coumarin derivatives from different starting materials. *Biomolecules*. 2020;10(1):151. doi:10.3390/biom10010151
- Weinmann I. History of the development and application of coumarin and coumarin related compounds. In: *Coumarins: Biology, Applications and Mode of Action*. John Wiley; 1997.
- Santos WH, Silva-Filho LC. NbCl₅-promoted synthesis of 4-aryl-3,4-dihydrocoumarins by multicomponent reaction. *Synthesis*. 2012;44(21):3361-3365. doi:10.1055/s-0032-1317340
- Sethna SM, Shah NM. The chemistry of coumarins. *Chem Rev*. 1945;36(1):1-62. doi:10.1021/cr60113a001
- Li Z, Kong D, Liu Y, Li M. Pharmacological perspectives and molecular mechanisms of coumarin derivatives against virus disease. *Genes Dis*. 2022;9(1):80-94. doi:10.1016/j.gendis.2021.03.007
- Sharifi-Rad J, Cruz-Martins N, López-Jornet P, et al. Natural coumarins: exploring the pharmacological complexity and underlying molecular mechanisms. *Oxid Med Cell Longev*. 2021;2021(8):6492346. doi:10.1155/2021/6492346
- Bisi A, Cappadone C, Rampa A, et al. Coumarin derivatives as potential antitumor agents: growth inhibition, apoptosis induction and multidrug resistance reverting activity. *Eur J Med Chem*. 2017;127(2):577-585. doi:10.1016/j.ejmech.2017.01.020
- Dai H, Huang M, Qian J, et al. Excellent antitumor and antimetastatic activities based on novel coumarin/pyrazole oxime hybrids. *Eur J Med Chem*. 2019;166(3):470-479. doi:10.1016/j.ejmech.2019.01.070
- Liu Y-P, Yan G, Guo J-M, et al. Prenylated coumarins from the fruits of *Manilkara zapota* with potential anti-inflammatory effects and anti-HIV activities. *J Agric Food Chem*. 2019;67(43):11942-11947. doi:10.1021/acs.jafc.9b04326
- Liu Y-P, Yan G, Xie Y-T, et al. Bioactive prenylated coumarins as potential anti-inflammatory and anti-HIV agents from *Clausena lenis*. *Bioorg Chem*. 2020;97(4):103699. doi:10.1016/j.bioorg.2020.103699
- Xu Z, Chen Q, Zhang Y, Liang C. Coumarin-based derivatives with potential anti-HIV activity. *Fitoterapia*. 2021;150(4):104863. doi:10.1016/j.fitote.2021.104863
- Estrada-Soto S, González-Trujano ME, Rendón-Vallejo P, Arias-Durán L, Ávila-Villarreal G, Villalobos-Molina R. Antihypertensive and vasorelaxant mode of action of the ethanol-soluble extract from *Tagetes lucida* Cav. aerial parts and its main bioactive metabolites. *J Ethnopharmacol*. 2021;266(2):113399. doi:10.1016/j.jep.2020.113399
- Revankar HM, Bukhari SNA, Kumar GB, Qin H-L. Coumarins scaffolds as COX inhibitors. *Bioorg Chem*. 2017;71(4):146-159. doi:10.1016/j.bioorg.2017.02.001
- Al-Warhi T, Sabt A, Elkaeed EB, Eldehna WM. Recent advancements of coumarin-based anticancer agents: an up-to-date review. *Bioorg Chem*. 2020;103(10):104163. doi:10.1016/j.bioorg.2020.104163
- Cho YH, Kim JH, Park SM, Lee BC, Pyo HB, Park HD. New cosmetic agents for skin whitening from *Angelica dahurica*. *J Cosmet Sci*. 2006;57(1):11-21.
- Hussain MI, Syed QA, Khattak MNK, Hafez B, Reigosa MJ, El-Keblawy A. Natural product coumarins: biological and pharmacological perspectives. *Biologia*. 2019;74(7):863-888. doi:10.2478/s11756-019-00242-x
- Pagona G, Katerinopoulos HE, Tagmatarchis N. Synthesis, characterization, and photophysical properties of a carbon nanohorn-coumarin hybrid material. *Chem Phys Lett*. 2011;516(1-3):76-81. doi:10.1016/j.cplett.2011.09.055
- Donnelly DMX, Boland GM. Isoflavonoids and neoflavonoids: naturally occurring O-heterocycles. *Nat Prod Rep*. 1995;12(3):321-338. doi:10.1039/NP951200321
- Rahman A-U. *Bioactive Natural Products (Part C): V22*. Vol. 22. Elsevier; 2000.
- Dhooghe L, Maregesi S, Mincheva I, et al. Antiplasmodial activity of (I-3,II-3)-biflavonoids and other constituents from *Ormocarpum kirkii*. *Phytochemistry*. 2010;71(7):785-791. doi:10.1016/j.phytochem.2010.02.005
- Hokkanen J, Mattila S, Jaakola L, Pirttilä AM, Tolonen A. Identification of phenolic compounds from lingonberry (*Vaccinium vitis-idaea* L.), bilberry (*Vaccinium myrtillus* L.) and hybrid bilberry (*Vaccinium x intermedium* Ruthe L.) leaves. *J Agric Food Chem*. 2009;57(20):9437-9447. doi:10.1021/jf9022542
- Tabanca N, Pawar RS, Ferreira D, et al. Flavan-3-ol-phenylpropanoid conjugates from *Anemopaegma arvense* and their antioxidant activities. *Planta Med*. 2007;73(10):1107-1111. doi:10.1055/s-2007-981563
- Zhang X-f, Wang H-m, Song Y-l, et al. Isolation, structure elucidation, antioxidative and immunomodulatory properties of two novel dihydrocoumarins from *Aloe vera*. *Bioorg Med Chem Lett*. 2006;16(4):949-953. doi:10.1016/j.bmcl.2005.10.096
- Aguiar GP, Crevelin EJ, Dias HJ, et al. Electrospray ionization tandem mass spectrometry of labdane-type acid diterpenes. *J Mass Spectrom*. 2018;53(11):1086-1096. doi:10.1002/jms.4284
- Dias HJ, Bento MVB, da Silva ÉH, et al. Gas-phase fragmentation reactions of protonated cocaine: new details to an old story. *J Mass Spectrom*. 2018;53(3):203-213. doi:10.1002/jms.4053
- Dias HJ, Crevelin EJ, Palaretti V, Vessecchi R, Crotti AEM. Electrospray ionization tandem mass spectrometry of deprotonated dihydrobenzofuran neolignans. *Rapid Commun Mass Spectrom*. 2021;35(3):e8990. doi:10.1002/rcm.8990
- Dias HJ, Stefani R, Tomaz JC, Vessecchi R, Crotti AEM. Differentiation between 3,4- and 4,15-epoxyeudesmanolides by electrospray ionization tandem mass spectrometry. *J Anal Meth Chem*. 2017;2017(11):7921867. doi:10.1155/2017/7921867
- Heinke R, Franke K, Michels K, Wessjohann L, Ali NAA, Schmidt J. Analysis of furanocoumarins from Yemenite *Dorstenia* species by liquid chromatography/electrospray tandem mass spectrometry. *J Mass Spectrom*. 2012;47(1):7-22. doi:10.1002/jms.2017
- Liang X, Han X. Fragmentation pathways of synthetic and naturally occurring coumarin derivatives by ion trap and quadrupole time-of-flight mass spectrometry. *Rapid Commun Mass Spectrom*. 2015;29(17):1596-1602. doi:10.1002/rcm.7245
- Borkowski EJ, Cecati FM, Suvire FD, et al. Mass spectrometry and theoretical calculations about the loss of methyl radical from methoxylated coumarins. *J Mol Struct*. 2015;1093(8):49-58. doi:10.1016/j.molstruc.2015.03.007
- Sun C, Wang Y, Sun S, et al. Fragmentation pathways of protonated coumarin by ESI-QE-Orbitrap-MS/MS coupled with DFT calculations. *J Mass Spectrom*. 2020;55(5):e4496. doi:10.1002/jms.4496
- Santos WH, Siqueira MS, Silva-Filho LC. Synthesis of 4-aryl-3,4-dihydrocoumarin derivatives catalyzed by NbCl₅. *Quim Nova*. 2013;36(9):1303-1307. doi:10.1590/S0100-40422013000900005
- Frisch MJ, Trucks GW, Schlegel HB, Scuseria GE, Robb MA, Cheeseman JR, Montgomery Jr JA, Vreven T, Kudin KN, Burant JC, Millam JM, Iyengar SS, Tomasi J, Barone V, Mennucci B, Cossi M, Scalmani G, Rega N, Petersson GA, Nakajima T, Honda Y, Kitao O, Nakai H, Klene M, Li X, Knowlton JE, Hratchian HP, Cross JB, Bakken V, Adamo C, Jaramillo J, Gomperts R, Stratmann RE, Yazyev O, Austin AJ, Cammi R, Pomelli C, Ochterski JW, Ayala PY, Morokuma K, Voth GA, Salvador P, Dannenberg JJ, Zakrzewski VG, Dapprich S, Daniels AD, Strain MC, Farkas O, Malick DK, Rabuck AD, Raghavachari K, Foresman JB, Ortiz JV, Cui Q, Babou AG, Clifford S, Cioslowski J, Stefanov BB, Liu G, Liashenko A, Piskorz P, Komaromi I, Martin RL, Fox DJ, Keith T, Al-Laham A, Peng CY, Nanayakkara A,

- Challacombe M, Gill PMW, Johnson B, Chen W, Wong WW, Gonzalez C, Pople JA. Gaussian 03, revision C. 02. Wallingford, CT: Gaussian, Inc.; 2004.
34. Vessecchi R, Naal Z, Lopes JN, Galembeck SE, Lopes NP. Generation of naphthoquinone radical anions by electrospray ionization: solution, gas-phase, and computational chemistry studies. *J Phys Chem a*. 2011;115(21):5453-5460. doi:10.1021/jp202322n
35. Andrienko GA Chemcraft – graphical software for visualization of quantum chemistry computations [Computer program]. Version 2022: 2022.
36. Vessecchi R, Galembeck SE, Lopes NP, Nascimento PG, Crotti AEM. Application of computational quantum chemistry to chemical processes involved in mass spectrometry. *Quim Nova*. 2008;31(4):840-853. doi:10.1590/S0100-40422008000400026
37. Vessecchi R, Galembeck SE. Evaluation of the enthalpy of formation, proton affinity, and gas-phase basicity of γ -butyrolactone and 2-pyrrolidinone by isodesmic reactions. *J Phys Chem a*. 2008;112(17):4060-4066. doi:10.1021/jp800427q
38. Range K, Riccardi D, Cui Q, Elstner M, York DM. Benchmark calculations of proton affinities and gas-phase basicities of molecules important in the study of biological phosphoryl transfer. *Phys Chem Chem Phys*. 2005;7(16):3070-3079. doi:10.1039/B504941E
39. Demarque DP, Crotti AEM, Vessecchi R, Lopes JL, Lopes NP. Fragmentation reactions using electrospray ionization mass spectrometry: an important tool for the structural elucidation and characterization of synthetic and natural products. *Nat Prod Rep*. 2016;33(3):432-455. doi:10.1039/C5NP00073D
40. McQuarrie DA. *Statistical Mechanics*. Harper & Row; 1976.
41. McLuckey SA. Principles of collisional activation in analytical mass spectrometry. *J Am Soc Mass Spectrom*. 1992;3(6):599-614. doi:10.1016/1044-0305(92)85001-Z
42. Dias HJ, Baguevard M, Crevelin EJ, et al. Gas-phase fragmentation reactions of protonated benzofuran-and dihydrobenzofuran-type neolignans investigated by accurate-mass electrospray ionization tandem mass spectrometry. *J Mass Spectrom*. 2019;54(1):35-46. doi:10.1002/jms.4304
43. Crotti AEM, Lopes JLC, Lopes NP. Triple quadrupole tandem mass spectrometry of sesquiterpene lactones: a study of goyazensolide and its congeners. *J Mass Spectrom*. 2005;40(8):1030-1034. doi:10.1002/jms.877
44. Dias HJ, Vieira TM, Crevelin EJ, Donate PM, Vessecchi R, Crotti AEM. Fragmentation of 2-arylbenzofuran derivatives by electrospray ionization tandem mass spectrometry. *J Mass Spectrom*. 2017;52(12):809-816. doi:10.1002/jms.4024
45. Henderson W, McIndoe JS. *Mass Spectrometric of Inorganic and Organometallic Compounds: Tools, Techniques, Tips*. John Wiley & Sons Inc.; 2005. doi:10.1002/0470014318
46. Demireva M, Armentrout PB. Relative energetics of the gas phase protomers of *p*-aminobenzoic acid and the effect of protonation site on fragmentation. *J Phys Chem a*. 2021;125(14):2849-2865. doi:10.1021/acs.jpca.0c11540
47. Acázar JJ, Márquez E, García-Río L, et al. Changes in protonation sites of 3-styryl derivatives of 7-(dialkylamino)-aza-coumarin dyes induced by cucurbit[7]uril. *Front Chem*. 2022;10:870137. doi:10.3389/fchem.2022.870137
48. Bouchoux G. Gas-phase basicities of polyfunctional molecules. Part 4: carbonyl groups as basic sites. *Mass Spectrom Rev*. 2015;34(5):493-534. doi:10.1002/mas.21416
49. Hunter EP, Lias SG. Evaluated gas phase basicities and proton affinities of molecules: an update. *J Phys Chem Ref Data Monogr*. 1998;27(3):413-656. doi:10.1063/1.556018
50. Mason RS, Böhme DK, Jennings KRJ. Gas-phase basicities of halogenotoluenes. *J Chem Soc, Faraday Trans 1*. 1982;78(6):1943-1952. doi:10.1039/F19827801943
51. Bohme D, Stone J, Mason R, Stradling R, Jennings K. A determination of proton-transfer equilibrium constants in benzene/halobenzene mixtures at various temperatures using a high-pressure ion source. *Int J Mass Spectrom Ion Phys*. 1981;37(3):283-296. doi:10.1016/0020-7381(81)80050-2
52. Kemister G, Pross A, Radom L, Taft RW. A theoretical approach to substituent effects. Examination of phenoxides and anilides as models for benzyl anions. *J Org Chem*. 1980;45(6):1056-1060. doi:10.1021/jo01294a028
53. Golden R, Stock L. Evidence for the dipolar field effect. *J Am Chem Soc*. 1966;88(24):5928-5929. doi:10.1021/ja00976a041
54. Mota CJA. Efeito de Campo. *Quim Nova*. 1987;10(4):295-297.
55. Sleno L, Volmer DAJ. Ion activation methods for tandem mass spectrometry. *J Mass Spectrom*. 2004;39(10):1091-1112. doi:10.1002/jms.703
56. Boyd R, Somogyi A. The mobile proton hypothesis in fragmentation of protonated peptides: a perspective. *J Am Soc Mass Spectrom*. 2010;21(8):1275-1278. doi:10.1016/j.jasms.2010.04.017
57. Reis A, Augusti R, Eberlin MN. A general, most basic rule for ion dissociation: protonated molecules. *J Mass Spectrom*. 2024;59(3):e5003. doi:10.1002/jms.5003
58. Attygalle AB, Xia H, Pavlov J. Influence of ionization source conditions on the gas-phase protomer distribution of anilinium and related cations. *J Am Soc Mass Spectrom*. 2017;28(8):1575-1586. doi:10.1007/s13361-017-1640-0
59. Sartori LR, Vessecchi R, Humpf HU, Da Costa FB, Lopes NP. A systematic investigation of the fragmentation pattern of two furanoheliangolide C-8 stereoisomers using electrospray ionization mass spectrometry. *Rapid Commun Mass Spectrom*. 2014;28(7):723-730. doi:10.1002/rcm.6839
60. Tureček F, Chen X. Protonated adenine: tautomers, solvated clusters, and dissociation mechanisms. *J Am Soc Mass Spectrom*. 2005;16(10):1713-1726. doi:10.1016/j.jasms.2005.06.010
61. Konermann L, Metwally H, McAllister RG, Popa V. How to run molecular dynamics simulations on electrospray droplets and gas phase proteins: basic guidelines and selected applications. *Methods*. 2018;144(7):104-112. doi:10.1016/j.ymeth.2018.04.010
62. Lettow M, Mucha E, Manz C, et al. The role of the mobile proton in fucose migration. *Anal Bioanal Chem*. 2019;411(3):4637-4645. doi:10.1007/s00216-019-01657-w
63. Sun F, Liu R, Zong W, Tian Y, Wang M, Zhang P. A unique approach to the mobile proton model: influence of charge distribution on peptide fragmentation. *J Phys Chem B*. 2010;114(19):6350-6353. doi:10.1021/jp911772q
64. Concannon S, Ramachandran VN, Smyth WF. A study of the electrospray ionisation of selected coumarin derivatives and their subsequent fragmentation using an ion trap mass spectrometer. *Rapid Commun Mass Spectrom*. 2000;14(14):1157-1166. doi:10.1002/1097-0231(20000730)14:1430.CO:2-V
65. Zhou Y, Zou X, Liu X, Peng S-I, Ding L-S. Multistage electrospray ionization mass spectrometric analyses of sulfur-containing iridoid glucosides in *Paederia scandens*. *Rapid Commun Mass Spectrom*. 2007;21(8):1375-1385. doi:10.1002/rcm.2965
66. Justino GC, Borges CM, Florêncio MH. Electrospray ionization tandem mass spectrometry fragmentation of protonated flavone and flavonol aglycones: a re-examination. *Rapid Commun Mass Spectrom*. 2009;23(2):237-248. doi:10.1002/rcm.3869
67. Menga H-C, Zhuc S, Fana Y-H, et al. Discovery of prenylated dihydrostilbenes in *Glycyrrhiza uralensis* leaves by UHPLC-MS using

neutral loss scan. *Ind Crop Prod.* 2020;152:112557. doi:[10.1016/j.indcrop.2020.112557](https://doi.org/10.1016/j.indcrop.2020.112557)

68. Lufshitz C. Tropylium ion formation from toluene: solution of an old problem in organic mass spectrometry. *Acc Chem Res.* 1994;27(5):138-144. doi:[10.1021/ar00041a004](https://doi.org/10.1021/ar00041a004)

SUPPORTING INFORMATION

Additional supporting information can be found online in the Supporting Information section at the end of this article.

How to cite this article: Dias HJ, Santos WH, Filho LCS, et al. Electrospray ionization tandem mass spectrometry of 4-aryl-3,4-dihydrocoumarins. *J Mass Spectrom.* 2024;59(7):e5062. doi:[10.1002/jms.5062](https://doi.org/10.1002/jms.5062)